Observational Study

Medicine®

OPEN

Distribution of somatic mutations of cancer-related genes according to microsatellite instability status in Korean gastric cancer

Joonhong Park, MD, PhD[a], Han Mo Yoo, MD[b], Woori Jang, MD, PhD[a], Soyoung Shin, MD, PhD[a], Myungshin Kim, MD, PhD[a], Yonggoo Kim, MD, PhD[a], Seung-Woo Lee, MD, PhD[c], Jeong Goo Kim, MD, PhD[b,*]

Abstract

In studies of the molecular basis of gastric cancer (GC), microsatellite instability (MSI) is one of the key factors. Somatic mutations found in GC are expected to contribute to MSI-high (H) tumorigenesis. We estimated somatic mutation distribution according to MSI status in 52 matched pair GC samples using the Ion Torrent Ion S5 XL with the AmpliSeq Cancer Hotspot panel.

Seventy-five (9.8%) somatic variants consisting of 34 hotspot mutations and 41 other likely pathogenic variants were identified in 34 GC samples. The *TP53* mutations was most common (35%, 26/75), followed by *EGFR* (8%, 6/75), *HNF1A* (8%, 6/75), *PIK3CA* (8%, 6/75), and *ERBB2* (5%, 4/75). To determine MSI status, 52 matched pair samples were estimated using 15 MSI markers. Thirty-nine MS stable (S), 5 MSI-low (L), and 8 MSI-H were classified. GCs with MSI-H tended to have more variants significantly compared with GCs with MS stable (MSS) and MSI-L (standardized J-T statistic = 3.161 for number of variants; $P = .002$). The mean number of all variants and hotspot mutations per tumor samples only in GCs with MSI-H were 3.9 (range, 1–6) and 1.1 (range, 0–3), respectively. Whereas, the mean number of all variants and hotspot mutations per tumor samples only in GCs with MSS/MSI-L were 1 (0–5)/0.8 (0–1) and 0.5 (0–3)/0.8 (0–1), respectively.

In conclusion, GC with MSI-H harbored more mutations in genes that act as a tumor suppressor or oncogene compared to GC with MSS/MSI-L. This finding suggests that the accumulation of MSIs contributes to the genetic diversity and complexities of GC. In addition, targeted NGS approach allows for detection of common and also rare clinically actionable mutations and profiles of comutations in multiple patients simultaneously. Because GC shows distinctive patterns related to ethnics, further studies pertaining to different racial/ethnic groups or cancer types may reinforce our investigations.

Abbreviations: GC = gastric cancer, MSI = microsatellite instability, MSI-H = MSI-high, MSI-L = MSI-low, MSS = microsatellite stable.

Keywords: AmpliSeq Cancer Hotspot panel, gastric cancer, microsatellite instability, next-generation sequencing

1. Introduction

Gastric cancer (GC) is currently the third leading cause of global cancer-related death, and is particularly prevalent in Asia.[1] Gastric adenocarcinoma, the most common type of GC, is heterogeneous and its incidence and cause varies widely with geographical regions, gender, ethnicity, and diet. Achieving a detailed molecular understanding of GC pathogenesis is pivotal to improving patient outcomes. The identification of genomic alterations may provide insight into the mechanisms for oncogenic gastric pathways and is important to identify a tumor marker in GC.[2–6]

Updated studies on GC molecular profiling have revealed heterogeneous characteristics for GC and have defined the subtypes on the basis of genomic basis, gene expression, and amplification patterns.[6–8] The Cancer Genome Atlas recently published results of a comprehensive study of GC, which provides an invaluable resource upon which to interpret other related GC findings. A molecular classification scheme in that study defined 4 major genomic subtypes of GC: Epstein–Barr virus (EBV)-infected tumors, microsatellite instability (MSI) tumors, genomically stable tumors, and chromosomal instability (CIN) tumors. Identification of these subtypes links the molecular alterations with clinical phenotypes and disease progression, providing a roadmap for patient stratification and trials of targeted therapies. According to gene expression patterns, some recent studies have classified GCs into molecular subtypes that show differences in the molecular and genetic features and chemotherapeutic sensitivity.[9,10] Importantly, the distinct salient genomic features of molecular subtypes will hopefully provide a guide to targeted agents that should be evaluated in clinical trials for distinct populations of GC patients. Several comprehensive studies describe that GC is associated with driver alterations, including gene mutations,[11,12] somatic copy number

Editor: Simona Gurzu.

The authors acknowledge the financial support of the Catholic Medical Center Research Foundation made in the program year of 2014.

The authors have no conflicts of interest to disclose.

[a] Department of Laboratory Medicine, [b] Division of Gastrointestinal Surgery, Department of Surgery, [c] Division of Gastroenterology, Department of Internal Medicine, College of Medicine, The Catholic University of Korea, Seoul, Republic of Korea.

[*] Correspondence: Jeong Goo Kim, Division of Gastrointestinal Surgery, Department of Surgery, Daejeon St. Mary's Hospital, College of Medicine, The Catholic University of Korea, 64 Daeheung-ro, Jung-gu, Daejeon 34943, Republic of Korea (e-mail: kalgs@catholic.ac.kr).

Medicine (2017) 96:25(e7224)

Received: 21 February 2017 / Received in final form: 23 May 2017 / Accepted: 30 May 2017

http://dx.doi.org/10.1097/MD.0000000000007224

alterations,[13,14] structural variants, epigenetic changes,[15] and transcriptional changes.[16–18] Certain driver alterations can also be associated with specific GC subtypes and the major forms of genomic instability observed in GC are CIN and MSI tumors.[19] MSI is defined as alterations in the lengths of microsatellites due to deletion or insertion of repeating units to produce novel length alleles in tumor DNA when compared with the normal/germline DNA from the same individual. When mismatch repair (MMR) genes, including mutL homolog 1 (MLH1) and mutS homolog 2 (MSH2), are inactivated, replication errors include insertions or deletions of bases within microsatellite regions.[20]

Next-generation sequencing (NGS), also known as high-throughput massively parallel sequencing, can detect multiple gene variants simultaneously, allowing for the precise diagnosis of a tumor at the genetic level. NGS generates many sequences across numerous targets and numerous patient samples in the same reaction and in a single instrument run, which reduces cost compared to Sanger sequencing. NGS promises to bridge this gap by allowing for simultaneous mutation detection in multiple exons from multiple genes in multiple patient samples.[21,22] NGS platforms offer an increased breadth of testing at a lower cost and without compromising assay performance and turn-around times in the clinical setting.[23,24] NGS analysis have shown that 15% to 20% of GCs are characterized by MSI.[25]

Several studies[11,16,26] have characterized mutation profiles in Korean GC; however, somatic mutations of cancer-related genes according to MSI status have not been studied in clinical samples. Here, we present our experience with targeted semiconductor using the Ion Torrent Ion S5 XL with the AmpliSeq Cancer Hotspot panel v2 to estimate somatic mutation distribution according to MSI status in GC; this assay covers 2855 COSMIC-cited hot spot mutations in 50 cancer-related genes.

2. Materials and methods

2.1. Samples and DNA isolation

A total of 52 primary gastric tumor tissues and paired normal tissues were obtained from surgically dissected patients with GC between 1999 to 2016 at the Daejeon St. Mary's Hospital, Daejeon, Republic of Korea. The results of immunohistochemical staining for MMR protein expression, such as MLH1 and MSH2, revealed that 13 of these tumors exhibited defective DNA MMR, while 39 presented proficient MMR proteins.[27] Each area of the tissue representing the "tumor" (highest numbers of cancer cells identified) and "normal" (no malignant tissue present) was microdissected separately, not to be contaminated by each other. Genomic DNA was extracted from microdissected tissue samples using the QIAmp DNeasy Blood and Tissue kit (Qiagen, Hilden, Germany) according to tissue protocol. Nucleic acid quality and quantity were assessed using a Nano-Drop 1000 spectrophotometer (NanoDrop Technologies, Wilmington, DE) and agarose gel electrophoresis. DNA concentration was determined using the Broad range Qubit DNA kit and Qubit 2.0 Fluorometer (Life Technologies, Carlsbad, CA). The study protocol was approved by the Institutional Review Board of The Catholic University of Korea, including written informed consent for clinical and molecular analyses.

2.2. Library preparation

AmpliSeq libraries were generated using the Ion AmpliSeq Library Kit 2.0 and the Ion AmpliSeq Cancer Hotspot Panel v2 (Life Technologies). This panel contains 207 primer pairs in a single tube and surveys hotspot regions including up to 2855 COSMIC mutations of 50 oncogenes and tumor suppressor genes, with wide coverage of the *KRAS*, *BRAF*, and *EGFR* genes. Included in this panel are primers for the amplification of regions of the following 50 genes: *ABL1*, *AKT1*, *ALK*, *APC*, *ATM*, *BRAF*, *CDH1*, *CDKN2A*, *CSF1R*, *CTNNB1*, *EGFR*, *ERBB2*, *ERBB4*, *EZH2*, *FBXW7*, *FGFR1*, *FGFR2*, *FGFR3*, *FLT3*, *GNA11*, *GNAS*, *GNAQ*, *HNF1A*, *HRAS*, *IDH1*, *JAK2*, *JAK3*, *IDH2*, *KDR*, *KIT*, *KRAS*, *MET*, *MLH1*, *MPL*, *NOTCH1*, *NPM1*, *NRAS*, *PDGFRA*, *PIK3CA*, *PTEN*, *PTPN11*, *RB1*, *RET*, *SMAD4*, *SMARCB1*, *SMO*, *SRC*, *STK11*, *TP53*, and *VHL*. Multiplex PCR was amplified using 10 ng genomic DNA with a premixed primer pool and Ion AmpliSeq HiFi master mix (Ion AmpliSeq Library Kit 2.0). The PCR amplicons were treated with 2 μL FuPa reagent to partially digest the primer sequences and phosphorylate the amplicons. The amplicons were ligated to adapters with the diluted barcodes of the Ion Xpress Barcode Adapters kit (Life Technologies). The adapter-ligated amplicons (library) were purified using the Agencourt AMPure XP reagent (Beckman Coulter, Brea, CA). Amplified libraries were assessed for quality (size and concentration) using a model 2100 bioanalyzer (Agilent Technologies, Santa Clara, CA) following the equipment's standard protocol. The ideal concentration for 1 sequence reaction on the One Touch instrument was between 8 and 16 pmol/L.

2.3. Emulsion PCR

The clonal amplification of the barcoded DNA library (The AmpliSeq libraries) onto the ion spheres (ISPs) was carried out using emulsion PCR following standard Ion Torrent protocols and the subsequent isolation of ISPs with DNA was conducted using Ion OneTouch 200 Template Kit v2 DL and Ion OneTouch ES (Life Technologies) according to the manufacturer's instructions. The polyclonal percentage and quality of the enriched, template-positive ISPs was determined using the Ion Sphere Quality Control Kit (Life Technologies). Samples with polyclonal percentage $<30\%$ and enriched, template-positive ISPs $> 80\%$ were subjected for sequencing on the Ion Torrent Ion S5 XL.

2.4. Sequencing

Enriched ISPs were loaded onto 540 chips taking 26 matched tumor and normal samples on a single chip per sequencing run. Ion Torrent Ion S5 XL sequencing was performed on the Ion 540 Kit-Chef (2 sequencing runs per initialization) and following the standard protocol. Sequencing was performed using 500 flow runs that generated approximately 200 bp reads.

2.5. Bioinformatic analysis

Raw signal data from sequencing runs from the Ion Torrent Ion S5 XL were automatically transferred to the Torrent Server Hosting the Torrent Suite Software that processed the raw voltage semiconductor sequencing data into DNA base calls. The pipeline included signaling processing, base calling, quality score assignment, adapter trimming, read mapping to 19 reference human genomes, quality control of mapping quality, coverage analysis with downsampling, and variant calling. Identification of variants was performed by the Ion Torrent Variant Caller plug-in and Ion Reporter software v5.2 (Life Technologies). Coverage maps were generated using the coverage analysis plug-in.

Torrent Variant Caller v5.2 was used for alignment and variant detection. The variant caller parameter setting was AmpliSEq Exome Tumor Normal v1 (5.2) Total Variants. Following data analysis, annotation of single-nucleotide variants, insertions, deletions, and splice site alterations was performed by the Ion Reporter Software (Life Technologies). Sequence data were visually confirmed with the Integrative Genomics Viewer (IGV) and any sequence, alignment, or variant call error artifacts were discarded. Hot spot mutations found in the 52 matched tumor and normal samples were compared to validate mutations listed in the Catalogue Of Somatic Mutations In Cancer (COSMIC). In addition, widely established computational prediction methods were applied to other than Hot spot mutations in this study. Evolution-based sequence information included the Sorting Intolerant From Tolerant (SIFT, http://sift.jcvi.org/) based on the degree of conservation of amino acid residues in sequence alignments derived from closely related sequences, collected through PSI-BLAST and the Grantham score that attempts to predict the distance between 2 amino acids, in an evolutionary sense.[28] Polymorphism Phenotyping v2 (PolyPhen-2, http://genetics.bwh.harvard.edu/pph2/) was used to predict the possible impact of an amino acid substitution on the structure and function of a human protein using straightforward physical and comparative considerations.

2.6. MSI analysis

To determine the MSI status in 52 GC samples, MSI analysis was performed using 15 different mono- and dinucleotide microsatellite markers. Eight mononucleotide markers consist of BAT25, BAT26, BAT40, BAT-RII, NR21, NR22, NR24, and NR27. Seven dinucleotide markers include D2S123, D5S346, D17S250, D17S261, D17S520, D18S34, and D18S58. Fifteen MSI markers were divided into groups of 5 and coamplified in 3 reaction tubes (1 group of 5 per tube). Allelic sizes to match the tumor and normal samples were compared and considered to be MSI unstable if there was a shift of 3 bp or more in the tumor allele.[29] All tumors with 1 or more unstable markers were regarded as carrying some degree of instability and were defined as MSI and MS stable (MSS) when there were no unstable markers. The cutoff for classification was applied on the basis of the threshold of about 40% that is commonly used to discriminate MSI-H (high) and MSI-L (low) tumors.[30]

2.7. Statistical analyses

Only patients with valid, exact clinicopathological characteristics were included in the statistical analysis. Since the tumor size, depth of tumor invasion, lymph node (LN) involvement, and disease stage was treated as an ordinal variable, the Jonckheere–Terpstra test was used to compare the ordinal variables. Overall survival (OS) was defined as the time between diagnosis and death by any cause. The statistical analyses were then carried out using the MedCalc ver. 12.7.2 (MedCalc software, Mariakerke, Belgium) and a $P < .05$ was considered to be statistically significant.

3. Results

3.1. Clinicopathological characteristics

The median age of the patients was 65.5 years (range 34–84) and the male to female ratio was 1.65. The most common tumor site in the stomach was distal (n = 28), followed by middle (n = 16), and proximal (n = 6). All tumors were diagnosed as GC; the vast majority were Borrmann 3 (n = 31), followed by EGC IIb (n = 7) and Borrmann 4 (n = 4) based on gross type. The most common Lauren classification was intestinal (n = 21), followed by mixed (n = 14), and diffuse (n = 12) type. According to the Japanese classification, tubular (n = 25) and tubulopapillary (n = 23) types were frequent. No metastasis was found; the disease stage was I (n = 17), II (n = 14), and III (n = 21). Clinicopathological characteristics of the 52 GCs are provided in Table 1.

3.2. Results of interest regions covered by the AmpliSeq Cancer Hotspot panel

The AmpliSeq Cancer Hotspot panel consists of 207 amplicons, which examines 2855 mutations in 50 commonly mutated oncogenes and tumor suppressor genes. Presently, the average of Q20 bases per sample were sequenced (Q20 = Phred quality score of 20; base call accuracy of 99%) and the median of >Q20 bases was 170,640,400 (range, 69,833,168–348,107,992). The median total numbers of bases was 186,030,778 (range, 75,324,153–376,373,688), the median of reads was 1,627,422 (range, 659,686–3,296,967), the median of mapped reads was 1,612,050 (range, 650,180–3,258,476), the median of mean read length was 114 bp (range, 104–121), the median of on target rate (%) was 97.1 (range, 80.9–99.4), the median of mean depth was 7,246 (range, 2,712–15,153), and the median of mean coverage uniformity (>20% mean coverage, %) was 99.9 (range, 90.1–100).

3.3. Spectrum of pathogenic and likely pathogenic somatic variants

In total, we obtained 767 variants from 52 matched pair samples. Of these, 692 variants were identified in both tumor and normal samples. The mean number of all variants per tumor and normal samples were 14.8 (range, 8–22) and 13.3 (range, 7–20), respectively. The mean number of hotspot mutations per tumor and normal samples was 2 (range, 0–5) and 1.3 (range, 0–5), respectively. Ion AmpliSeq v2 revealed somatic mutations in 34 of the 52 GC matched pair samples. After filtering out variants identified only in tumor samples, 75 (9.8%) variants comprising 34 hotspot mutations and 41 pathogenic variants that were likely other than hotspot mutations were selected (Tables 2 and 3). Seventy-five somatic variants in 21 genes were detected with a mean of 2.2 variants (range, 1–6) per sample. Categorized according to mutated genes, *TP53* mutations were most common (35%, 26/75), followed by *EGFR* (8%, 6/75), *HNF1A* (8%, 6/75), *PIK3CA* (8%, 6/75), *ERBB2* (5%, 4/75), *ATM* (4%, 3/75), *FGFR2* (4%, 3/75), *CDKN2A* (4%, 3/75), *FLT3* (3%, 2/75), *PDGFRA* (3%, 2/75), *PTEN* (3%, 2/75), *RB1* (3%, 2/75), *STK11* (3%, 2/75), *APC* (1%, 1/75), *FBXW7* (1%, 1/75), *MET* (1%, 1/75), *NOTCH1* (1%, 1/75), *RET* (1%, 1/75), *SMAD4* (1%, 1/75), *SMO* (1%, 1/75), and *UBALD1* (1%, 1/75). The mutations detected in *EGFR*, *ERBB2*, *PIK3CA*, and *STK11* were considered potentially actionable.[31,32] Such actionable mutations were identified in 12 patients, most commonly in EGFR (8%, 6/75), *PIK3CA* (8%, 6/75), *ERBB2* (5%, 4/75), and *STK11* (3%, 2/75). Classified according by mutation types, the majority of pathogenic and likely pathogenic variants identified only in tumor samples were missense (65%, 49/75) followed by frameshift (28%, 21/75), nonsense (4%, 3/75), and silent (3%, 2/75) mutations (Fig. 1). We also identified the cooccurrence of the most frequently altered and clinically significant genes. Not

Table 1

Clinicopathological characteristics of 52 gastric cancers according to microsatellite instability status.

Clinicopathological characteristics	Total (n = 52, 100%)	MSS (n = 39, 75%)	MSI-L (n = 5, 10%)	MSI-H (n = 8, 15%)
Age, y; median (range)	65.5 (34–84)	61 (47–83)	58 (34–73)	73.5 (66–84)
Males (%)	33 (63.5)	25 (64.1)	4 (80)	4 (50)
Tumor location (%)				
Proximal	6 (11.5)	4 (10.3)	2 (40)	0 (0)
Middle	16 (30.8)	15 (38.5)	1 (20)	0 (0)
Distal	28 (53.8)	18 (46.2)	2 (40)	8 (100)
Whole	2 (3.8)	2 (5.1)	0 (0)	0 (0)
Gross type (%)				
EGC I	3 (5.8)	2 (5.1)	0 (0)	1 (12.5)
EGC IIa	0 (0)	0 (0)	0 (0)	0 (0)
EGC IIb	7 (13.5)	5 (12.8)	0 (0)	2 (25)
EGC IIc	3 (5.8)	1 (2.6)	1 (20)	1 (12.5)
EGC III	0 (0)	0 (0)	0 (0)	0 (0)
Borrmann 1	0 (0)	0 (0)	0 (0)	0 (0)
Borrmann 2	3 (5.8)	3 (7.7)	0 (0)	0 (0)
Borrmann 3	31 (59.6)	23 (59)	4 (80)	4 (50)
Borrmann 4	4 (7.7)	4 (10.3)	0 (0)	0 (0)
Unclassified	1 (1.9)	1 (2.6)	0 (0)	0 (0)
Lauren classification (%)				
Intestinal	21 (40.4)	15 (38.5)	1 (20)	5 (62.5)
Diffuse	12 (23.1)	10 (25.6)	1 (20)	1 (12.5)
Mixed	14 (26.9)	9 (23.1)	3 (60)	2 (25)
Unclassified	5 (9.6)	5 (12.8)	0 (0)	0 (0)
Japanese classification (%)				
Papillary	1 (1.9)	1 (2.6)	0 (0)	0 (0)
Tubular, moderately differentiated	25 (48.1)	18 (46.2)	2 (40)	5 (62.5)
Tubulopapillary	23 (44.2)	17 (43.6)	3 (60)	3 (37.5)
Mucinous	1 (1.9)	1 (2.6)	0 (0)	0 (0)
Signet-ring cell	1 (1.9)	1 (2.6)	0 (0)	0 (0)
Others	1 (1.9)	1 (2.6)	0 (0)	0 (0)
Differentiation (%)				
Differentiated	26 (50)	19 (48.7)	2 (40)	5 (62.5)
Undifferentiated	26 (50)	20 (51.3)	3 (60)	3 (37.5)
Tumor size (cm); median (range)	4 (1–25)	4 (1–25)	5 (1–7.5)	3 (2–7)
<4 (%)	24 (46.2)	17 (43.6)	2 (40)	5 (62.5)
≥4 (%)	28 (53.8)	22 (56.4)	3 (60)	3 (37.5)
Depth of tumor invasion (%)				
T1	17 (32.7)	12 (30.8)	1 (20)	4 (50)
T2	5 (9.6)	5 (12.8)	0 (0)	0 (0)
T3	12 (23.1)	10 (25.6)	1 (20)	1 (12.5)
T4	18 (34.6)	12 (30.8)	3 (60)	3 (37.5)
Lymph node involvement (%)				
N0	25 (48.1)	17 (43.6)	2 (40)	6 (75)
N1	5 (9.6)	3 (7.7)	1 (20)	1 (12.5)
N2	8 (15.4)	7 (17.9)	1 (20)	0 (0)
N3	14 (26.9)	12 (30.8)	1 (20)	1 (12.5)
Presence of metastasis (%)				
M0	52 (100)	39 (100)	5 (100)	8 (100)
M1	0 (0)	0 (0)	0 (0)	0 (0)
Stage (%)				
I	17 (32.7)	12 (30.8)	1 (20)	4 (50)
II	14 (26.9)	10 (25.6)	2 (40)	2 (25)
III	21 (40.4)	17 (43.6)	2 (40)	2 (25)
IV	0 (0)	0 (0)	0 (0)	0 (0)
R status (%)				
R0	46 (88.5)	36 (92.3)	3 (60)	7 (87.5)
R1	4 (7.7)	2 (5.1)	1 (20)	1 (12.5)
R2	2 (3.8)	1 (2.6)	1 (20)	0 (0)
Type of operation (%)				
Total gastrectomy	16 (30.8)	12 (30.8)	4 (80)	0 (0)
Subtotal gastrectomy	36 (69.2)	27 (69.2)	1 (20)	8 (100)
Lymphadenectomy (%)				
D1	8 (15.4)	4 (10.3)	3 (60)	1 (12.5)
D2 or more	44 (84.6)	35 (89.7)	2 (40)	7 (87.5)
Adjuvant chemotherapy (%)				
No	32 (61.5)	23 (59)	3 (60)	6 (75)
Yes	20 (38.5)	16 (41)	2 (40)	2 (25)
Survival period, mo; median (range)	16.3 (8.7–216.1)	17.1 (8.7–216.1)	12.4 (9.2–114.1)	11 (9.3–41.8)
Outcome (%)				
Alive	36 (69.2)	26 (66.7)	4 (80)	6 (75)
Dead	6 (11.5)	5 (12.8)	1 (20)	0 (0)
Unknown	10 (19.2)	8 (20.5)	0 (0)	2 (25)
Variant* (%)	34 (65.4)	22 (56.4)	4 (80)	8 (100)
Silent	2 (3.8)	1 (2.5)	0 (0)	1 (12.5)
Missense	30 (57.7)	18 (46.2)	4 (80)	8 (100)
Nonsense	3 (5.8)	2 (5.1)	0 (0)	1 (12.5)
Frameshift	14 (26.9)	9 (23.1)	0 (0)	5 (62.5)

MSI-H = microsatellite highly unstable, MSI-L = microsatellite lowly unstable, MSS = microsatellite stable, other = other likely pathogenic variants than hotspot mutations.

* Patients with more than 1 variant were counted as 1.

Table 2

Hotspot somatic mutations in 34 matched pair gastric cancers.

ID	Gene	Nucleotide change	Amino acid change	Type	Freq. (%)	Depth* (×)	COSMIC ID
I02	*TP53*	c.586C>T	p.Arg196*	Nonsense	57.1	1997	COSM99668
I05	*TP53*	c.730G>A	p.Gly244Ser	Missense	67.9	1999	COSM10941
I06	*TP53*	c.832C>A	p.Pro278Thr	Missense	8.3	2000	COSM43697
I08	*TP53*	c.844C>T	p.Arg282Trp	Missense	49.5	1929	COSM10704
I10	*TP53*	c.476C>T	p.Ala159Val	Missense	6.7	1995	COSM11148
I10	*ERBB2*	c.2264T>C	p.Leu755Ser	Missense	4.5	2000	COSM14060
I10	*ERBB2*	c.2524G>A	p.Val842Ile	Missense	7.8	1999	COSM14065
I14	*TP53*	c.77G>A	p.Arg26His	Missense	24.6	1992	COSM220780
I20	*PIK3CA*	c.3140A>G	p.His1047Arg	Missense	14.9	2000	COSM94986
I20	*ERBB2*	c.2524G>A	p.Val842Ile	Missense	12.2	2000	COSM14065
I21	*TP53*	c.844C>T	p.Arg282Trp	Missense	33.4	1945	COSM99925
I22	*TP53*	c.723delC	p.Cys242fs	Out-of-frame	17.9	1996	COSM6530
I23	*TP53*	c.638G>A	p.Arg213Gln	Missense	5.3	1988	COSM10735
I26	*TP53*	c.614A>T	p.Tyr205Phe	Missense	23	1992	COSM11351
I29	*TP53*	c.818G>A	p.Arg273His	Missense	40.6	1995	COSM10660
I34	*TP53*	c.743G>A	p.Arg248Gln	Missense	70.3	1989	COSM10662
I35	*TP53*	c.586C>T	p.Arg196*	Nonsense	29.5	1980	COSM99668
I37	*PIK3CA*	c.1636C>G	p.Gln546Glu	Missense	9.5	1922	COSM6147
I37	*PIK3CA*	c.1637A>G	p.Gln546Arg	Missense	5.4	1925	COSM12459
I37	*TP53*	c.536A>G	p.His179Arg	Missense	53	1998	COSM10889
I40	*TP53*	c.526T>A	p.Cys176Ser	Missense	54.9	1997	COSM44146
I45	*TP53*	c.245G>A	p.Arg82His	Missense	42.6	2000	COSM99024
I46	*TP53*	c.844C>T	p.Arg282Trp	Missense	10.6	1971	COSM99925
I47	*PIK3CA*	c.3140A>T	p.His1047Leu	Missense	27.2	1999	COSM94987
I48	*PIK3CA*	c.1637A>G	p.Gln546Arg	Missense	17.1	1925	COSM12459
I49	*TP53*	c.460G>A	p.Gly154Ser	Missense	22.2	1996	COSM43692
I50	*PIK3CA*	c.3140A>G	p.His1047Arg	Missense	35.6	1999	COSM94986
I51	*TP53*	c.463C>T	p.Arg155Trp	Missense	27.7	1994	COSM120006
I52	*PDGFRA*	c.2472C>T	p.(=)	Silent	50	1997	COSM22413
I52	*PDGFRA*	c.2524_2535del12	p.I843_D846delIMHD	In-frame	38	1953	COSM737
I53	*TP53*	c.817C>T	p.Arg273Cys	Missense	14.6	1999	COSM99933
I54	*TP53*	c.743G>T	p.Arg248Leu	Missense	34.7	1985	COSM6549
I55	*PTEN*	c.797delA	p.Lys267fs	Out-of-frame	14.3	1996	COSM87314
I56	*TP53*	c.488A>G	p.Tyr163Cys	Missense	26.3	1951	COSM10808

COSMIC = Catalogue of Somatic Mutations in Cancer.

* The depth of coverage distributions was downsampled to a maximum depth of 2000.

surprisingly, *TP53* mutations cooccurred most commonly with mutations of other genes. Among 6 patients with *EGFR* mutations, 3 also had a coexisting *PIK3CA* (patient I37), *ERBB2* (patient I08), and *STK11* (patient I41) mutations. Interestingly, the 3 patients harbored compound heterozygous mutations of *PIK3CA* (patient I37), *TP53* (patient I45), and *ERBB2* (patient I10).

3.4. Associations between clinicopathological characteristics and MSI status

To determine MSI status, 52 matched pair samples were estimated using 15 MSI markers. Thirty-nine MSS and 13 unstable MSI were classified. Out of the 13 samples with defective MMR protein expression, 8 (62%) were classified as MSI-H with instability at ≥6 markers and 5 (38%) were MSI-L with instability at ≤5 markers. Jonckheere–Terpstra test results showed that when MSI status went from stable to highly unstable, tumor size, depth of tumor invasion, LN involvement, and disease stage tended to decrease. These observations were not statistically significant (standardized J-T statistic = −0.587 for tumor size, 0.274 for depth of tumor invasion, −1.485 for LN involvement, and −0.881 for stage; $P = .557$, .784, .138, and .378, respectively). However, GCs with MSI-H tended to have significantly more variants compared with GCs with MSS/MSI-L (3.161 for number of variants; $P = .002$) (Fig. 2). The mean number of all variants and hotspot mutations per tumor samples only in GCs with MSI-H were 3.9 (range, 1–6) and 1.1 (range, 0–3), respectively (Table 4). Meanwhile, 36 patients were alive and 6 had died at the time of the analysis. Ten were lost to follow-up during the study period. The median follow-up duration was 16.3 months (range, 8.7–216.1). Within the cohort of survival outcome that were available, all 6 with MSI-H were alive, while 5 with MSS and 1 with MSI-L had died.

4. Discussion

GC is characterized by a high level of biological heterogeneity, with each patient exhibiting a distinct genetic and molecular profile. Studies of the molecular basis of GC have led to the recognition of 4 major genomic subtypes of GC.[10] MSI is one of the key factor in several cancers, including colorectal, endometrial, and GC. Microsatellite mutations found in these cancers are expected to contribute to MSI-H tumorigenesis.[33] Depending on the type and number of MSI markers analyzed, widely variable results have been reported for the frequency of MSI-H in GC: 11.7% to 33.8% in Asian[34–36] and 16.3% to 25.2% in European[37–40] population. Recent exome sequencing of gastric adenocarcinoma showed that samples with unstable MSI had an average of 31.61 somatic mutations

Table 3

Other likely pathogenic somatic variants than hotspot mutations in 34 matched pair gastric cancers.

ID	Gene	Nucleotide change	Amino acid change	Type	Freq. (%)	Depth (×)	SIFT	Grantham	PolyPhen-2	rs ID
I04	*FGFR2*	c.1626T>G	p.Ile542Met	Missense	22.67	2000	0.01	10.0	0.86	na
I04	*ATM*	c.8223A>T	p.Arg2741Ser	Missense	13.46	1995	0.07	110	0.209	na
I04	*RB1*	c.596delT	p.Leu199fs	Out-of-frame	37.36	1989	na	na	na	na
I04	*TP53*	c.247G>A	p.Ala83Thr	Missense	17.09	1989	0.78	58	0	na
I04	*NOTCH1*	c.7426G>A	p.Val2476Met	Missense	17.72	1870	0.3	21	0.003	na
I04	*CDKN2A*	c.393C>T	p.(=)	Silent	11.2	2000	na	na	na	na
I06	*ATM*	c.7938delT	p.Asn2646fs	Out-of-frame	13.89	2000	na	na	na	na
I06	*HNF1A*	c.745delT	p.Ser249fs	Out-of-frame	22.86	1998	na	na	na	na
I06	*UBALD1*	c.317C>T	p.Ser106Leu	Missense	23.9	1646	0	145	0.965	na
I06	*EGFR*	c.2405delT	p.Val802fs	Out-of-frame	35	1890	na	na	na	na
I08	*ERBB2*	c.2408_2409delATinsTC	p.Tyr803Phe	In-frame	26.09	1998	0.32	22	0.531	na
I08	*EGFR*	c.278delT	p.Leu93fs	Out-of-frame	18.60	1870	na	na	na	na
I08	*CDKN2A*	c.275A>C	p.Asp92Ala	Missense	19.35	2000	0.04	126	0.999	na
I10	*HNF1A*	c.745delT	p.Ser249fs	Out-of-frame	17.86	1998	na	na	na	na
I10	*FLT3*	c.1404delA	p.Asp469fs	Out-of-frame	23.53	1999	na	na	na	na
I10	*SMAD4*	c.1108G>A	p.Val370Ile	Missense	14.81	1998	0	29	0.997	na
I11	*PTEN*	c.762A>T	p.Lys254Asn	Missense	7.11	1983	0	94	0.999	na
I11	*TP53*	c.683_686delACTG	p.Asp228fs	Out-of-frame	12.4	1984	na	na	na	na
I14	*FGFR2*	c.1626T>G	p.Ile542Met	Missense	27.78	1999	0.01	10	0.86	na
I16	*EGFR*	c.2399A>G	p.Asp800Gly	Missense	22.22	1870	0	94	1	na
I20	*ATM*	c.8155C>T	p.Arg2719Cys	Missense	11.51	1999	0	180	1	rs138526014
I26	*HNF1A*	c.745delT	p.Ser249fs	Out-of-frame	17.14	1990	na	na	na	na
I29	*APC*	c.4561delG	p.Glu1521fs	Out-of-frame	23.69	1870	na	na	na	na
I37	*EGFR*	c.278delT	p.Leu93fs	Out-of-frame	30.77	1953	na	na	na	na
I41	*RET*	c.2636delA	p.Asn879fs	Out-of-frame	42.38	1987	na	na	na	na
I41	*EGFR*	c.2405delT	p.Val802fs	Out-of-frame	11.76	1972	na	na	na	na
I41	*SMO*	c.542A>C	p.Glu181Ala	Missense	44.44	1998	0.02	107	0.934	na
I41	*HNF1A*	c.745delT	p.Ser249fs	Out-of-frame	20	1994	na	na	na	na
I41	*FLT3*	c.1404delA	p.Asp469fs	Out-of-frame	18.52	2000	na	na	na	na
I41	*STK11*	c.1096T>A	p.Phe366Ile	Missense	66.67	2000	0.01	21	0.925	na
I43	*CDKN2A*	c.275A>G	p.Asp92Gly	Missense	14.71	2000	0	94	0.997	na
I43	*FGFR2*	c.1218delG	p.Lys407fs	Out-of-frame	66.67	2000	na	na	na	na
I43	*TP53*	c.325T>G	p.Phe109Val	Missense	28.8	1595	0	50	0.999	na
I44	*MET*	c.3712G>A	p.Val1238Ile	Missense	22.98	2000	0	29	0.995	rs121913670
I44	*EGFR*	c.2399A>G	p.Asp800Gly	Missense	31.25	1998	0	94	1	na
I45	*HNF1A*	c.745delT	p.Ser249fs	Out-of-frame	18.6	1983	na	na	na	na
I45	*TP53*	c.524G>A	p.Arg175His	Missense	15.11	1984	0.09	29	0.632	rs28934578
I45	*STK11*	c.1096T>A	p.Phe366Ile	Missense	57.14	1998	0.01	21	0.925	na
I49	*FBXW7*	c.1322G>A	p.Arg441Gln	Missense	24.11	2000	0	43	1	na
I55	*HNF1A*	c.608G>A	p.Arg203His	Missense	10.15	1998	0	29	1	na
I55	*RB1*	c.1060C>T	p.Gln354Ter	Nonsense	4.15	1416	na	na	na	na

na = not available, SIFT = Sorting Intolerant From Tolerant, rs ID = reference SNP ID number.

per megabase of DNA, whereas MSS GCs had an average of 3.29, a difference of approximately 10-fold.[41] Moreover, a recent comprehensive genome- and transcriptome-wide study of Korean GCs supported the suggestion that mutations in 3′ untranslated regions (UTRs) influence gene expression in MSI-H tumors.[16] Several *cis*- or *trans*-elements of the UTRs might fail to regulate gene functions like stability and activity if the mutations alter RNA sequences or structure.[16] This finding suggests that aberrant expression of genes may create a growth or survival advantage for MSI-H GC. In our study, the survive analysis between MSI-H and MSS/MSI-L was not suitable because of the small sample size (n = 52) and short median follow-up duration of 16.3 months. A recent meta-analysis for GC with unstable MSI with good prognosis, although heterogeneity in recent studies was present.[42] MSI-H indicated by double negativity of MLH-1 and MSH-2 was not implicated in the pathogenesis of the early-onset GCs.[43] Altered epidemiology and effects of chemotherapy are potential causes of the heterogeneity. On the other hand, MSI-H tumors were associated with a good prognosis in Stage II and III GC when patients were treated by surgery alone, and the benefits of MSI-H status were attenuated by chemotherapy.[44]

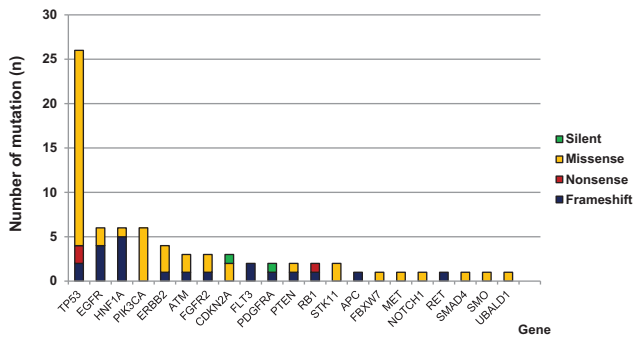

Figure 1. Distribution of pathogenic and likely pathogenic somatic variants identified in 34 gastric cancers.

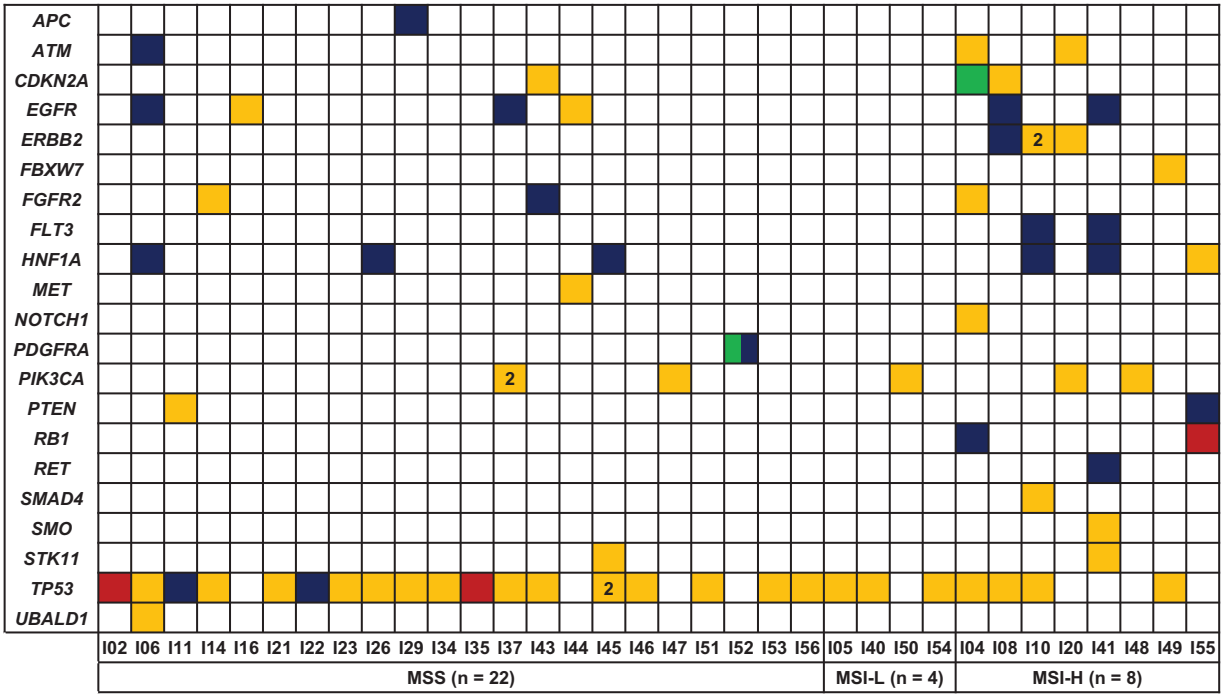

Figure 2. Spectrum of pathogenic and likely pathogenic somatic variants according to MSI status. Blue box, frameshift mutation; green box, silent mutation; red box, nonsense mutation; yellow box, missense mutation.

Postreplication MMR is an important mechanism for maintaining microsatellite stability through the correction of base change mismatches and insertion/deletion events. MSI has length specificity, and the instability was driven mostly by deletion rather than insertion.[16] Premutational intermediates are identified and processed by heterodimers of the MutS and MutL family of proteins.[45] The number of candidate genes with deletion mutations is significantly greater than previously reported, implying that the accumulation of MSIs contributes to the genetic complexities of GC.[16] Colorectal cancer (CRC) patients with defective MMR tumors have distinct clinical and pathologic features, thus this finding highlights the importance of MSI testing in early-stage disease where patients can be potentially cured by surgery alone or combined with adjuvant chemotherapy.[46] Important in the biology of CRC are somatic mutations in the *KRAS* and *BRAF* oncogenes and the status of the DNA MMR system.[46,47] Recently, Gurzu et al[48] identified the molecular and immunohistochemical criteria that can be used to recognize the possible serrated pathway. Interestingly, we characterized GC with MSI-H containing more somatic variants than that with MSS and MSI-L (3.9 vs 1 and 0.8). The detection of multiple, cooccurring, potentially actionable mutations in an individual tumor represents an advance in molecular pathology with possible significant clinical, therapeutic, and research implications based on the different combinations of mutations.[32] Even though the mutational spectra for genes with high mutational frequencies are quite different between MSI-H GC and CRC, our analysis of mutations associated with MSI in GCs will provide further information about discrete molecular pathways, which may explain the difference. The number of candidate cancer-related genes mutated in cases of GC with MSI-H is significantly greater than those in GCs with MSS or MSI-L, implying that the accumulation of MSIs contributes to the genetic complexities of GC. The present findings will enhance our understanding of gastric tumorigenesis in MSI-H cancers. Establishing a consensus for defining MSI in GC is a laudable aim for further studies.

Because distinct somatic mutations have been identified in each human cancer, it is essential to classify and characterize the molecular alterations underlying GC for improving more personalized and precision therapies.[49] Once the molecular profile of a tumor is known, the appropriate use of targeted clinical therapies or eligibility for clinical trials can be determined. It is desirable to have the ability to analyze several genes simultaneously to assess for the presence of a known clinically

Table 4

Mean number of variant per matched-pair samples according to MSI status in 52 matched pair gastric cancers.

	Tumor			Normal			Tumor only (tumor–normal)		
	Variants	Hotspot	Other	Variants	Hotspot	Other	Variants	Hotspot	Other
Total (n = 52)	14.8 (8–22)	2 (0–5)	12.8 (7–20)	13.3 (7–0)	1.3 (0–5)	12 (7–16)	1.4 (0–6)	0.7 (0–3)	0.8 (0–6)
MSS (n = 39)	14.3 (8–21)	1.9 (0–5)	12.4 (7–18)	13.3 (7–20)	1.4 (0–5)	11.9 (7–16)	1 (0–5)	0.5 (0–3)	0.5 (0–4)
MSI-L (n = 5)	12.8 (10–16)	1.6 (1–3)	11.2 (8–5)	12 (9–15)	0.8 (0–2)	11.2 (8–15)	0.8 (0–1)	0.8 (0–1)	0
MSI-H (n = 8)	18.1 (13–22)	2.4 (1–)	15.8 (10–20)	14.3 (12–17)	1.3 (0–2)	13 (10–15)	3.9 (1–6)	1.1 (0–3)	2.8 (0–6)

MSI-H = microsatellite highly unstable, MSI-L = microsatellite lowly unstable, MSS = microsatellite stable, other = other likely pathogenic variants than hotspot mutations.

actionable variant in a tumor. To understand and develop new therapeutics and treat GC more effectively, it is essential to profile the individual cancer genome and MSI status and dissect the oncogenic mechanisms that regulate the progression of GC, which may form the foundation for individualized, tailored therapy. The molecular profiling using NGS technologies offers advantages to detect somatic cancer genome alterations in accuracy, sensitivity, and speed that can make a significant impact, enabling the assessment of all potentially causative genes at the same time.[21] In this study, we estimated the utility of the Ion Torrent Ampliseq technology for clinical genotyping of GC. Using this targeted NGS panel in our cohort, we frequently identified *TP53* (48%, 25/52 vs 4.6% and 27%) and *PIK3CA* (10%, 5/52 vs 5.1% and 5.6%) mutations similar to previous reports about Korean GCs,[11,26] whereas higher frequency of *EGFR* (12%, 6/52 vs 0% and 0%) and *HNF1A* (12%, 6/52 vs 0% and 0%) mutations were evident. This may be due to different GC subtypes, histological type, the TNM staging, degree of metastasis, use of matched pair samples, or the design of gene panel even though the same Korean ethnicity was studied. We identified rare mutations that would be specific therapeutic significance. Examples include detection of *EGFR* c.278delT (p.Leu93fs), c.2399A>G (p.Asp800Gly), c.2405delT (p.Val802fs); *ERBB2* c.2264T>C (p.L755S), c.2524G>A (p.V842I), c.2408_2409delATinsTC (p.Tyr803Phe); *PIK3CA* c.3140A>G (p.H1047R), c.1636C>G (p.Q546E), c.1637A>G (p.Q546R), c.3140A>T (p.H1047L), c.1637A>G (p.Q546R), c.3140A>G (p.H1047R), and *STK11* c.1096T>A (p.Phe366Ile). There were no recurrent mutations in the *BRAF*, *EGFR*, *ERBB2*, *PDGFRA*, *PTEN*, and *RET* genes, for which targeted drug therapies are available.

Although NGS technology is useful for identifying and characterizing the somatic mutations that accrue in GC and provides novel potential targets for molecular therapies, there are several limitations for GC.[50] First, the previous reports were studied at single institutes using specific subtypes of GC in small sample sizes, rather than all types of GCs. Thus, a large-scaled multiinstitutional study for GC using optimized NGS for GC is required. Second, functional study on potential driver or actionable genes discovered by NGS should be conducted to prove the functional consequences of genomic alterations.[51,52] To date, 2 candidate driver mutated genes (*TP53* and *ARID1A*) have been simultaneously identified by exome sequencing.[41,53,54] Despite these limitations, NGS remains a powerful molecular profiling approach, which enables ultra-deep sequencing of the primary tumor lesion to detect rare subclones, and low-depth sequential tumor characterization to identify dominant clones.[55,56]

In conclusion, GC with MSI-H harbored more mutations in genes that act as a tumor suppressor or oncogene compared to GC with MSS/MSI-L. This finding suggests that the accumulation of MSIs contributes to the genetic diversity and complexities of GC. In addition, targeted NGS approach allows for detection of common and also rare clinically actionable mutations and profiles of comutations in multiple patients simultaneously. Because GC shows distinctive patterns related to ethnics, further studies pertaining to different racial/ethnic groups or cancer types may reinforce our investigations.

Acknowledgments

We would like to specially thank Chang Hyeon Lee and Keun-Joon Park of Thermo Fisher Scientific for providing technical support about Ion Torrent NGS works in this study.

References

[1] Ferlay J, Soerjomataram I, Ervik M, et al. Cancer Incidence and Mortality Worldwide. *In: IARC CancerBase no 11 International Agency for Research on Cancer, Lyon, France*. 2013.
[2] Kim C, Mulder K, Spratlin J. How prognostic and predictive biomarkers are transforming our understanding and management of advanced gastric cancer. Oncologist 2014;19:1046–55.
[3] Nakamura J, Tanaka T, Kitajima Y, et al. Methylation-mediated gene silencing as biomarkers of gastric cancer: a review. World J Gastroenterol 2014;20:11991–2006.
[4] Yamamoto H, Watanabe Y, Maehata T, et al. An updated review of gastric cancer in the next-generation sequencing era: insights from bench to bedside and vice. World J Gastroenterol 2014;20: 3927–37.
[5] Jiang C, Chen X, Alattar M, et al. MicroRNAs in tumorigenesis, metastasis, diagnosis and prognosis of gastric cancer. Cancer Gene Therapy 2015;22:291–301.
[6] Ishimoto T, Baba H, Izumi D, et al. Current perspectives toward the identification of key players in gastric cancer microRNA dysregulation. Int J Cancer 2016;138:1337–49.
[7] Hudler P. Challenges of deciphering gastric cancer heterogeneity. World J Gastroenterol 2015;21:10510–27.
[8] Yu Y. A new molecular classification of gastric cancer proposed by Asian Cancer Research Group (ACRG). Transl Gastrointest Cancer 2015; 5:55–7.
[9] Lei Z, Tan IB, Das K, et al. Identification of molecular subtypes of gastric cancer with different responses to PI3-kinase inhibitors and 5-fluorouracil. Gastroenterology 2013;145:554–65.
[10] The Cancer Genome Atlas Research NetworkComprehensive molecular characterization of gastric adenocarcinoma. Nature 2014;513:202–9.
[11] Lee J, van Hummelen P, Go C, et al. High-throughput mutation profiling identifies frequent somatic mutations in advanced gastric adenocarcinoma. PLoS ONE 2012;7:e38892.
[12] Nagarajan N, Bertrand D, Hillmer AM, et al. Whole-genome reconstruction and mutational signatures in gastric cancer. Genome Biol 2012;13:R115.
[13] Deng N, Goh LK, Wang H, et al. A comprehensive survey of genomic alterations in gastric cancer reveals systematic patterns of molecular exclusivity and co-occurrence among distinct therapeutic targets. Gut 2012;61:673–84.
[14] Dulak AM, Schumacher SE, Van Lieshout J, et al. Gastrointestinal adenocarcinomas of the esophagus, stomach, and colon exhibit distinct patterns of genome instability and oncogenesis. Cancer Res 2012; 72:4383–93.
[15] Sukawa Y, Yamamoto H, Nosho K, et al. Alterations in the human epidermal growth factor receptor 2-phosphatidylinositol 3-kinase-v-Akt pathway in gastric cancer. World J Gastroenterol 2012;18:6577–86.
[16] Yoon K, Lee S, Han T-S, et al. Comprehensive genome- and transcriptome-wide analyses of mutations associated with microsatellite instability in Korean gastric cancers. Genome Res 2013;23:1109–17.
[17] Liu J, McCleland M, Stawiski EW, et al. Integrated exome and transcriptome sequencing reveals ZAK isoform usage in gastric cancer. Nat Commun 2014;5:3830.
[18] Sulahian R, Casey F, Shen J, et al. An integrative analysis reveals functional targets of GATA6 transcriptional regulation in gastric cancer. Oncogene 2014;33:5637–48.
[19] Ottini L, Falchetti M, Lupi R, et al. Patterns of genomic instability in gastric cancer: clinical implications and perspectives. Ann Oncol 2006;17 (suppl 7):vii97–102.
[20] Veigl ML, Kasturi L, Olechnowicz J, et al. Biallelic inactivation of hMLH1 by epigenetic gene silencing, a novel mechanism causing human MSI cancers. Proc Natl Acad Sci U S A 1998;95:8698–702.
[21] Metzker ML. Sequencing technologies—the next generation. Nat Rev Genet 2010;11:31–46.
[22] Quail MA, Smith M, Coupland P, et al. A tale of three next generation sequencing platforms: comparison of Ion Torrent, Pacific Biosciences and Illumina MiSeq sequencers. BMC Genomics 2012;13:341.
[23] Hadd AG, Houghton J, Choudhary A, et al. Targeted, high-depth, next-generation sequencing of cancer genes in formalin-fixed, paraffin-embedded and fine-needle aspiration tumor specimens. J Mol Diagn 2013;15:234–47.
[24] Tsongalis GJ, Peterson JD, de Abreu FB, et al. Routine use of the Ion Torrent AmpliSeq™ Cancer Hotspot Panel for identification of clinically actionable somatic mutations. Clin Chem Lab Med 2014;52:707–14.
[25] Tan P, Yeoh K-G. Genetics and molecular pathogenesis of gastric adenocarcinoma. Gastroenterology 2015;149:1153.e3–62.e3.

[26] Kim S, Lee J, Hong ME, et al. High-throughput sequencing and copy number variation detection using formalin fixed embedded tissue in metastatic gastric cancer. PLoS ONE 2014;9:e111693.
[27] Ewald J, Rodrigue C, Mourra N, et al. Immunohistochemical staining for mismatch repair proteins, and its relevance in the diagnosis of hereditary non-polyposis colorectal cancer. Br J Surg 2007;94:1020–7.
[28] Grantham R. Amino acid difference formula to help explain protein evolution. Science 1974;185:862–4.
[29] Bacher JW, Sievers CK, Albrecht DM, et al. Improved detection of microsatellite instability in early colorectal lesions. PLoS ONE 2015;10: e0132727.
[30] Tomlinson I, Halford S, Aaltonen L, et al. Does MSI-low exist? J Pathol 2002;197:6–13.
[31] Takeda M, Sakai K, Terashima M, et al. Clinical application of amplicon-based next-generation sequencing to therapeutic decision making in lung cancer. Ann Oncol 2015;26:2477–82.
[32] Tafe LJ, Pierce KJ, Peterson JD, et al. Clinical genotyping of non-small cell lung cancers using targeted next-generation sequencing: utility of identifying rare and co-mutations in oncogenic driver genes. Neoplasia 2016;18:577–83.
[33] Shin N, You KT, Lee H, et al. Identification of frequently mutated genes with relevance to nonsense mediated mRNA decay in the high microsatellite instability cancers. Int J Cancer 2011;128: 2872–80.
[34] Kim H, An JY, Noh SH, et al. High microsatellite instability predicts good prognosis in intestinal-type gastric cancers. J Gastroenterol Hepatol 2011;26:585–92.
[35] Fang WL, Chang SC, Lan YT, et al. Microsatellite instability is associated with a better prognosis for gastric cancer patients after curative surgery. World J Surg 2012;36:2131–8.
[36] An C, Choi IS, Yao JC, et al. Prognostic significance of CpG island methylator phenotype and microsatellite instability in gastric carcinoma. Clin Cancer Res 2005;11(2 Pt 1):656–63.
[37] Corso G, Pedrazzani C, Marrelli D, et al. Correlation of microsatellite instability at multiple loci with long-term survival in advanced gastric carcinoma. Arch Surg (Chicago, Ill: 1960) 2009;144:722–7.
[38] Falchetti M, Saieva C, Lupi R, et al. Gastric cancer with high-level microsatellite instability: target gene mutations, clinicopathologic features, and long-term survival. Hum Pathol 2008;39:925–32.
[39] Hayden JD, Cawkwell L, Quirke P, et al. Prognostic significance of microsatellite instability in patients with gastric carcinoma. Eur J Cancer (Oxford, England: 1990) 1997;33:2342–6.
[40] Beghelli S, de Manzoni G, Barbi S, et al. Microsatellite instability in gastric cancer is associated with better prognosis in only stage II cancers. Surgery 2006;139:347–56.
[41] Wang K, Kan J, Yuen ST, et al. Exome sequencing identifies frequent mutation of ARID1A in molecular subtypes of gastric cancer. Nat Genet 2011;43:1219–23.
[42] Choi YY, Bae JM, An JY, et al. Is microsatellite instability a prognostic marker in gastric cancer? A systematic review with meta-analysis. J Surg Oncol 2014;110:129–35.
[43] Gurzu S, Kadar Z, Sugimura H, et al. Gastric cancer in young vs old Romanian patients: immunoprofile with emphasis on maspin and mena protein reactivity. APMIS 2015;123:223–33.
[44] Kim SY, Choi YY, An JY, et al. The benefit of microsatellite instability is attenuated by chemotherapy in stage II and stage III gastric cancer: results from a large cohort with subgroup analyses. Int J Cancer 2015;137: 819–25.
[45] Shah SN, Hile SE, Eckert KA. Defective mismatch repair, microsatellite mutation bias, and variability in clinical cancer phenotypes. Cancer Res 2010;70:431–5.
[46] Kawakami H, Zaanan A, Sinicrope FA. Microsatellite instability testing and its role in the management of colorectal cancer. Curr Treat Options Oncol 2015;16:30.
[47] Chen W, Swanson BJ, Frankel WL. Molecular genetics of microsatellite-unstable colorectal cancer for pathologists. Diagn Pathol 2017;12:24.
[48] Gurzu S, Szentirmay Z, Toth E, et al. Serrated pathway adenocarcinomas: molecular and immunohistochemical insights into their recognition. PLoS ONE 2013;8:e57699.
[49] Xu Z, Huo X, Ye H, et al. Genetic mutation analysis of human gastric adenocarcinomas using ion torrent sequencing platform. PLoS ONE 2014;9:e100442.
[50] Liang H, Kim YH. Identifying molecular drivers of gastric cancer through next-generation sequencing. Cancer Lett 2013;340:241–6.
[51] Liang H, Cheung LW, Li J, et al. Whole-exome sequencing combined with functional genomics reveals novel candidate driver cancer genes in endometrial cancer. Genome Res 2012;22:2120–9.
[52] Wiegand KC, Hennessy BT, Leung S, et al. A functional proteogenomic analysis of endometrioid and clear cell carcinomas using reverse phase protein array and mutation analysis: protein expression is histotype-specific and loss of ARID1A/BAF250a is associated with AKT phosphorylation. BMC Cancer 2014;14:120.
[53] Cajuso T, Hanninen UA, Kondelin J, et al. Exome sequencing reveals frequent inactivating mutations in ARID1A, ARID1B, ARID2 and ARID4A in microsatellite unstable colorectal cancer. Int J Cancer 2014;135:611–23.
[54] Zang ZJ, Cutcutache I, Poon SL, et al. Exome sequencing of gastric adenocarcinoma identifies recurrent somatic mutations in cell adhesion and chromatin remodeling genes. Nat Genet 2012;44:570–4.
[55] Meric-Bernstam F, Mills GB. Overcoming implementation challenges of personalized cancer therapy. Nat Rev Clin Oncol 2012;9:542–8.
[56] Le Tourneau C, Delord JP, Goncalves A, et al. Molecularly targeted therapy based on tumour molecular profiling versus conventional therapy for advanced cancer (SHIVA): a multicentre, open-label, proof-of-concept, randomised, controlled phase 2 trial. Lancet Oncol 2015; 16:1324–34.